Density functional theory study of MnO by a hybrid functional approach

C. Franchini,* V. Bayer, and R. Podloucky
Institut für Physikalische Chemie, Universität Wien and Center for Computational Materials Science, Liechtensteinstrasse 22A, A-1090 Vienna, Austria

J. Paier and G. Kresse
Institut für Materialphysik, Universität Wien and Center for Computational Materials Science, Sensengasse 8, A-1090 Wien, Austria
(Received 8 February 2005; revised manuscript received 2 May 2005; published 19 July 2005)

The ground state properties of MnO are investigated using the plane wave based projector augmented wave technique and the so-called "parameter-free" hybrid functional approach PBE0 for the approximation of the exchange-correlation energy and potential. The insulating, antiferromagnetically ordered and rhombohedrally distorted B1 structure is found to be the most stable phase of MnO, consistent with experiment. The band gap of 4.02 eV, spin magnetic moment of 4.52 μ_B, optimized lattice parameter $a=4.40$ Å, rhombohedral distortion angle $\alpha=0.88^0$, density of states, and magnetic properties are all in good agreement with experiment. Results obtained from standard methods such as generalized gradient approximation (GGA), GGA+U and periodic Hartee-Fock are also reported for comparative purposes. In line with previous studies, our results suggest that the applied hybrid functional method PBE0, which combines 25% of the exact exchange with a generalized-gradient approximation, corrects the deficiency of semilocal density functionals and provides an accurate quantitative description of the structural, electronic, and magnetic properties of MnO without any adjustable parameter.

DOI: 10.1103/PhysRevB.72.045132 PACS number(s): 71.27.+a, 71.15.Ap, 75.30.Et

I. INTRODUCTION

Conventional density functional approximations introduced to evaluate the exchange-correlation energy, such as the local spin density (LSDA) and generalized gradient (GGA) approximations, are known to be inadequate to account for the electronic structure of materials with localized *d* orbitals, in particular for insulating, antiferromagnetic transition-metal oxides, for which incorrect band gaps, spectral weights, and magnetic moments are obtained. It has been indicated[1] that most of the difficulties of the LSDA may be due to the unphysical electronic self-interaction which induces a wrong treatment of the Coulomb interaction, the fundamental quantity for describing Mott insulators. Several approaches introducing corrections for localized states were suggested to overcome these limitations. The most widely used methods are the GW approximation,[2] the self-interaction correction (SIC),[3] and the LSDA+U[4] approach. Within SIC and GW the energy splitting between occupied and unoccupied states is treated by explicitly calculating the self-energy; within LSDA+U a term corresponding to the mean-field approximation of the Coulomb interaction is added which concomitantly influences the band splitting. An alternative remedy, which has recently attracted much interest, is the so-called hybrid functional approach[5] which consists of the mixture of the exact nonlocal Hartree-Fock (HF) exchange with standard local exchange-correlation functionals. It depends on three empirical parameters a_1, a_2, a_3, and has the general form,[6–8]

$$E_{xc}^{\mathrm{hyb}} = E_{xc}^{\mathrm{LSDA}} + a_1(E_x - E_x^{\mathrm{LSDA}}) + a_2\Delta E_x^{\mathrm{GGA}} + a_3\Delta E_c^{\mathrm{GGA}}. \tag{1}$$

In Eq. (1), E_{xc}^{LSDA} is the standard LSDA exchange-correlation energy, constructed to be correct in the uniform electron gas limit, and E_x is the exact HF exchange. The quantities $\Delta E_x^{\mathrm{GGA}}$ and $\Delta E_c^{\mathrm{GGA}}$ are the gradient corrections to LSDA for exchange and correlation, respectively, defined as $\Delta E^{\mathrm{GGA}} = E^{\mathrm{GGA}} - E^{\mathrm{LSDA}}$. Recently, Eq. (1) was reduced by Becke[9] to an expression with only one parameter,

$$E_{xc}^{\mathrm{hyb}} = E_{xc}^{\mathrm{GGA}} + a(E_x - E_x^{\mathrm{GGA}}). \tag{2}$$

The semiempirical parameter a is determined by an appropriate fit to experimental data, such as atomization energies, ionization potentials, and the total energy of atoms and molecules.[7,8] Although, in principle, this hybrid functional would require a material dependent parameter, Perdew *et al.*[7] rationalized the choice of $a=1/4$ by a coupling-constant integration. This *a priori* choice of the parameter a generates a class of "parameter-free" hybrid functionals (i.e., with the same number of parameters as the GGA constituents).

One of the most widely used hybrid functionals is the B3LYP approach,[8,10] which includes three empirical parameters to adjust the mixing according to Eq. (1), resulting in 20% HF exchange. It has been shown that this functional correctly reproduces not only the thermochemical properties of atoms and molecules (for which it has been designed) but also the ground state of strongly correlated electronic systems.[11–14] Nevertheless, in its original formulation, B3LYP provides magnetic coupling constants overestimated by about 50%. Deeper investigation[11,12,14,15] has shown that a better agreement between calculated and experimental exchange integrals is obtained when a larger portion of HF exchange is included, about 35% (Fock-35). However, the energy gaps found using Fock-35 turn out to be larger by about 50% than the experimental and B3LYP results.[11,14,15] Although both B3LYP and Fock-35 method provide a reliable description of the ground state properties of correlated

TABLE I. MnO: Calculated and experimental values for the energy gap Δ(eV), the spin magnetic moment $m(\mu_B)$, the $e_g - t_{2g}$ splitting Δ_v(eV), the lattice parameter a(Å), and the rhombohedral distortion angle α(degrees). The HF study has been performed for the undistorted B1 structure only. Experimental values are taken from references:

	PBE	PBE+U	PBE0	HF	B3LYP	SCGW	Model GW	SIC	HF	Expt.
		(This work)			(Ref. 12)	(Ref. 28)	(Ref. 29)	(Ref. 30)	(Ref. 42)	
Δ	1.44	2.03	4.02	12.6	3.92	3.5	4.2	4.0, 3.6	12.9	3.6–4.2[a,b]
m	4.31	4.69	4.52	4.7	4.73		4.52	4.49, 4.64	4.9	4.58,[c] 4.79[d]
Δ_v	1.3	3.0	1.7	3.9		1.7	1.6		~3.0	1.8,[e] 1.9[f]
a	4.37	4.48	4.40	4.38	4.50				4.53	4.43,[c] 4.4448[g]
					LSDA		GGA		HF	
					(Refs. 41 and 44)		(Refs. 43 and 44)		(Ref. 42)	
α	1.66	0.56	0.88		0.66,1.68		1.69,~2.0		0.47	0.62[h]

[a]Ref. 34
[b]Ref. 35
[c]Ref. 36
[d]Ref. 37
[e]Ref. 38
[f]Ref. 39
[g]Ref. 40
[h]Ref. 27

materials, the mixing parameter for the HF exchange largely effects the calculated properties and different percentages of HF exchange are needed to obtain more accurate results for different material properties.[14] Ciofini *et al.*[16] have recently shown that the "parameter-free" class of hybrid functionals [Eq. (2)] provide values for the coupling constants of the antiferromagnetic systems $KNiF_3$ and K_2NiF_4 in better agreement with experiment than B3LYP. Furthermore, Ciofini *et al.* tested three different "parameter-free" variants, B1LYP[17] (derived from B3LYP), mPW0[18] (derived from the Perdew-Wang functional) and PBE0[19,20] [which uses the the GGA type Perdew-Burke-Ernzerhof (PBE) functional[21]], and found that the best performance is provided by the PBE0 approach.

In the present report we exploit the hybrid functional PBE0 to investigate the ground state structural, electronic and magnetic properties of MnO. Based on the approach of Chawla and Voth[22] for the evaluation of the exact exchange, the PBE0 functional was implemented in the projector augmented wave (PAW)[23,24] version of the *Vienna ab initio Simulation Package* (VASP).[25] Details of the implementation are given elsewhere.[26] It should be noted, that within the framework of ground state DFT our results are strictly valid only for $T=0$ K. As we will show, the application of the "parameter-free" hybrid functional to a solid system correctly predicts the ground state properties of the correlated system MnO.

Below the Néel temperature of $T_N=118$ K, MnO is a type-II antiferromagnetic (AFM-II) insulator and crystallizes in a rhombohedrally distorted B1 structure with a distortion angle of $\alpha=0.62°$.[27] For temperatures $T>T_N$ the rock salt structure of the paramagnetic phase is undistorted. MnO has a long standing reputation of being a computational challenge because of the strong on-site Coulomb repulsion of the $3d$ states, and it has been widely studied both, experimentally and theoretically. To improve upon the inadequacy of conventional electronic structure schemes, many innovative techniques were applied to MnO, ranging from GW,[28] model GW,[29] SIC,[30,31] LSDA+U[32] to the B3LYP[12] approach. In the present work we calculate and compare results of the PBE0 functional, the conventional GGA functional PBE, the plane wave Hartree-Fock approach and of an LSDA+U method (PBE+U) in which the semilocal part is again described by PBE. A detailed comparison with existing theoretical and experimental reports will also be given. The paper is organized as follows. In Sec. II, we describe the computational method. In Sec. III, we present and discuss the results. Finally, in Sec. IV, we draw the conclusions.

II. METHOD AND COMPUTATIONAL DETAILS

First principles density functional theory calculations (PBE, PBE+U,[4,33] HF, and PBE0) have been performed using the PAW-based VASP code, within the generalized gradient spin density approximation to the DFT in the Perdew-Burke-Ernzerhof parameterization scheme. A well converged shape and volume minimization was reached, by means of evaluation of the stress tensor and forces, at an energy cutoff of 300 eV and a $4\times4\times4$ Monkhorst-Pack k-point grid. The calculation of the ground state properties, density of states (DOS) and band structures was refined using a denser $8\times8\times8$ k-mesh. We used valence electron configuration $3d^6\,4s^1$ and $2s^2\,p^4$ for the Mn and O pseudopotentials, respectively. Suitable supercells have been built to account for the different magnetic orderings considered. To make a reasonable choice for the on-site Coulomb interaction U and the exchange parameter J we made preliminary investigations varying U between 4 and 9 eV, maintaining the ratio $J=U/10$, and testing both the Dudarev[33] and Anisimov[4] LSDA+U approach, both schemes gave almost identical re-

TABLE II. PBE0 results for MnO: comparison of results for undistorted and distorted B1 structure. Units as in Table I.

	Δ	m	Δ_v	a
$\alpha=0$	3.96	4.52	1.6	4.44
$\alpha=0.88$	4.02	4.52	1.7	4.40

sults. It turned out that $U-J=6.0$ eV is the optimal choice, in agreement with constrained LSDA evaluations which resulted in $U=6.9$ eV and $J=0.86$ eV.[4]

III. RESULTS AND DISCUSSION

In Table I our calculated values for the energy gap Δ, spin magnetic moment m, band splitting Δ_v between the highest occupied e_g and t_{2g} levels, lattice parameter a, and rhombohedral distortion angle α of the most stable AFM-II phase are compared to available experimental data and other calculations. From the upper panel of this table one can deduce that the PBE0 values are in significantly better agreement with experiment than the PBE and PBE+U results, in particular for Δ and Δ_v with improvements very similar to the other methods which go beyond standard local functionals. As expected, the HF gap is much larger than the experimental one and our values agree rather well with previous estimations of Towler *et al.*,[42] a useful test which confirms the trustability of our approach also in the limit of 100% HF exchange. It should be noted that the data for B3LYP, GW, and SIC calculations refer to the undistorted B1 structure and–with the exception of B3LYP–are performed for the experimental lattice constant without any optimization. In the B3LYP calculations an energy minimization of the undistorted B1 structure has been performed, and it provides a lattice parameter that is slightly larger than the experimental value.

In order to analyze the effect of the lattice distortion within PBE0, we also investigated the undistorted B1 structure deriving a lattice parameter of $a_{B1}=4.44$ Å which is slightly larger than the value for the distorted structure of $a=4.40$ Å (see Table II). For the distorted B1 structure, the compression along the [111] direction slightly reduces the volume and enhances the insulating character, and as a consequence, the band splitting of $\Delta=4.02$ eV is slightly increased in comparison to the value of $\Delta_{B1}=3.96$ eV. The spin magnetic moment remains unchanged. The rhombohedral distortion can be studied also in terms of nearest-neighbors (NN) and next nearest-neighbors (NNN) magnetic interactions as defined for the Heisenberg spin Hamiltonian,[48]

$$H=\sum_{NN} J_1 \mathbf{S}_i \cdot \mathbf{S}_j + \sum_{NNN} J_2 \mathbf{S}_i \cdot \mathbf{S}_j. \tag{3}$$

A value of $J>0$ indicates ferromagnetic exchange, and $J<0$ marks antiferromagnetic interactions. We obtained the values of the exchange parameters by differences of total energies between various magnetic orderings. We have considered three different magnetic configurations: ferromagnetic (FM), type-I AFM, and type-II AFM. Neglecting quantum fluctuations and considering one formula unit one may write for the total AFM-II energies of the distorted (H_{dist}) and undistorted (H_{B1}) structure, and for the FM and AFM-I systems

$$H_{B1}=-3J_2S^2, \tag{4}$$

$$H_{dist}=-3J_1^{\uparrow\downarrow}S^2+3J_1^{\uparrow\uparrow}S^2-3J_2S^2, \tag{5}$$

$$H_{FM}=6J_1S^2+3J_2S^2, \tag{6}$$

$$H_{AFM-I}=-2J_1S^2+3J_2S^2, \tag{7}$$

The parameters $J_1^{\uparrow\downarrow}$ and $J_1^{\uparrow\uparrow}$ are the exchange integrals connecting adjacent (antiparallel) and in-plane (parallel) NN spins, respectively, and $S=\frac{5}{2}$ is the spin of the Mn^{2+} atom. Under the assumption of a volume conserving transition, the NNN distance and the NNN exchange interaction J_2 remain unchanged. This simplification is supported by the experimentally derived values[50,51] which show only a very small change of J_2 of 1.4% between the two phases, and also by our calculations yielding a negligible volume variation of 0.4%. This is obviously not true for the NN distance: upon compression, in fact, adjacent [111] planes move closer together and in-plane Mn atoms move further apart, giving rise to different sets of J_1 parameters, namely $J_1^{\uparrow\downarrow}$ and $J_1^{\uparrow\uparrow}$. From Eqs. (4) and (5) it follows that the transition lowers the energy if

$$H_{dist}-H_{B1}=(J_1^{\uparrow\uparrow}-J_1^{\uparrow\downarrow})3S^2<0, \tag{8}$$

which means $J_1^{\uparrow\uparrow}<J_1^{\uparrow\downarrow}$.

In Table III we list our calculated estimations for the exchange integrals along with previous theoretical and semi-

TABLE III. Compilation of theoretical and experimental values for exchange integrals in K. Paramaters $|J_1|$ and ΔJ are defined

	PBE	PBE+U	PBE0	HF	B3LYP	LSDA+U	LSDA		Semiempirical		
		(This work)			(Ref. 12)	(Ref. 44)	(Ref. 47)	(Refs. 45 and 46)	(Ref. 48)	(Ref. 49)	(Ref. 50)
J_1	17.6	8.2	11.5	2.7	9.80	9.3	18.8	24.5	10		
J_2	27.9	4.3	13.7	4.3	20.5	24.5	33.0	43.6	11	10.3	9.6
$J_1^{\uparrow\downarrow}$	20.7	8.7	12.8				21.3			10.	9.9
$J_1^{\uparrow\uparrow}$	14.3	7.7	10.6				16.4			7.9	7.5
$J_2/\|J_1\|$	1.6	0.5	1.2	1.6	2.1	2.6	1.8	1.8	1.1	1.2	1.1
ΔJ	3.2	0.5	1.1				3.0			1.1	1.2

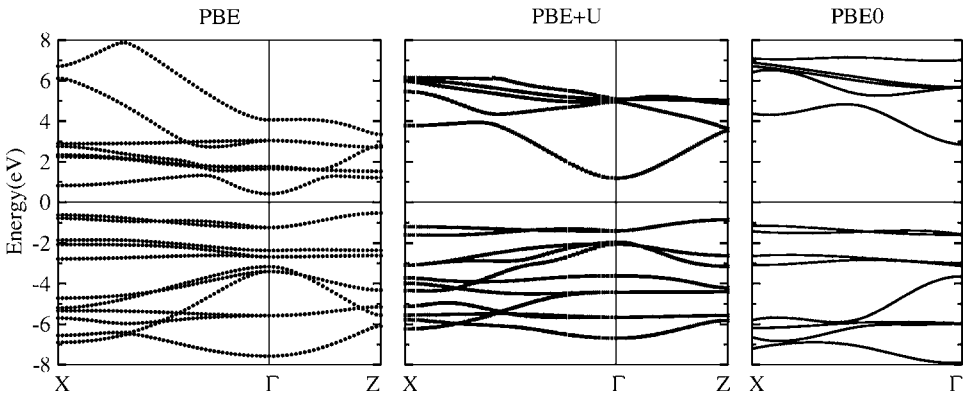

FIG. 1. Band structure for MnO, calculated within three different functionals, from left to right: PBE, PBE+U, and PBE0. The Γ-*Z* path is missing for PBE0 due to a computational restriction related to a *k*-points sampling.

empirical data. We note that all methods (with the exception of HF for which only the undistorted structure has been considered) fulfill the above condition of stabilization for the rhombohedral phase, in agreement with the recent work of Pask *et al.*[44] and with semiempirical evaluations. Application of PBE0 improves upon all previous studies, although residual deviations of about 30% with semiempirical values remain. In particular, application of PBE0 results in $J_2/|J_1| = 1.2$ and $\Delta J \equiv (J_1^{\uparrow\downarrow} - J_1^{\uparrow\uparrow})/2 = 1.1$ meV, in excellent agreement with the parameters derived from experiment,[52] $J_2/|J_1| = 1.0 \pm 0.1$, and also being consistent to semiempirical evaluations, in much better agreement than all other theoretical values. For the difference between $J_1^{\uparrow\uparrow}$ and $J_1^{\uparrow\downarrow}$ one may argue that due to the distortion the distance between adjacent [111] planes decreases, and consequentially, the NN exchange interaction between antiparallel spins–as described by $J_1^{\uparrow\downarrow}$–situated on different [111] planes is enhanced. In contrast, the distance between planar parallel spins gets larger upon the transition, and the NN planar magnetic interaction manifested in the parameter $J_1^{\uparrow\uparrow}$ decreases.

We finally discuss the electronic properties of MnO summarized in Figs. 1 and 2 displaying the band structure and the DOS, respectively. Although the arrangement of bands calculated for the three different functionals differs considerably, all methods predict the insulating character of MnO and ascribe it to the intermediate Mott-Hubbard/charge-transfer type of insulator (the top of the valence band is of mixed O 2*p*–Mn e_g character), with some distinctions: in the valence band the hybridization between O and Mn states is larger in PBE+U(45% O+55% Mn) and PBE0(25% O +75% Mn) than in PBE where the amount of oxygen is only about 10%, suggesting that a standard PBE treatment tends to describe MnO as a "Mott-Hubbard" small-band-gap insulator. The gap opens between this valence orbital and the unoccupied electronic states that are made up by a mixture of Mn and O 2*s* states hybridizing weakly with oxygen *p* states.

The major differences between the three methods arise from the size of the gap, the energy separation between unoccupied and occupied *d* states and the splitting Δ_v. As expected, the gap for PBE ($\Delta = 1.44$ eV) is much smaller than the experimental one in the range of 3.6–4.2 eV, while PBE0 provides the best value of 4.02 eV, which is due to the upward shift of the unoccupied Mn *d* states by about 3 eV. Within PBE+U we obtain the value $\Delta = 2.03$ eV for U–$J = 6.0$ eV. One could argue that in order to derive the experimental gap a larger value of U should be used. From the energy separation between the occupied and unoccupied t_{2g} and e_g states in the PBE0 calculations we derive a value of $U \approx 8$ eV, which is in fact larger than the value we used in the LDA+U case. Nevertheless, a further PBE+U calculation, now for $U = 8$ eV, provides a splitting of $\Delta = 2.2$ eV, still significantly smaller than experiment. Even a larger and unphysical value of $U = 15$ eV does not result in a significant improvement, the band gap is now ≈ 3 eV. In fact, the energy onset of the oxygen *p* conduction band, lying about 1.5 eV above the Fermi energy, and the top of the valence band remain almost unchanged with increasing U, making the gap almost independent of U, although a larger U shifts the occupied Mn *d* states and unoccupied Mn *d* states further downward and upward, respectively.

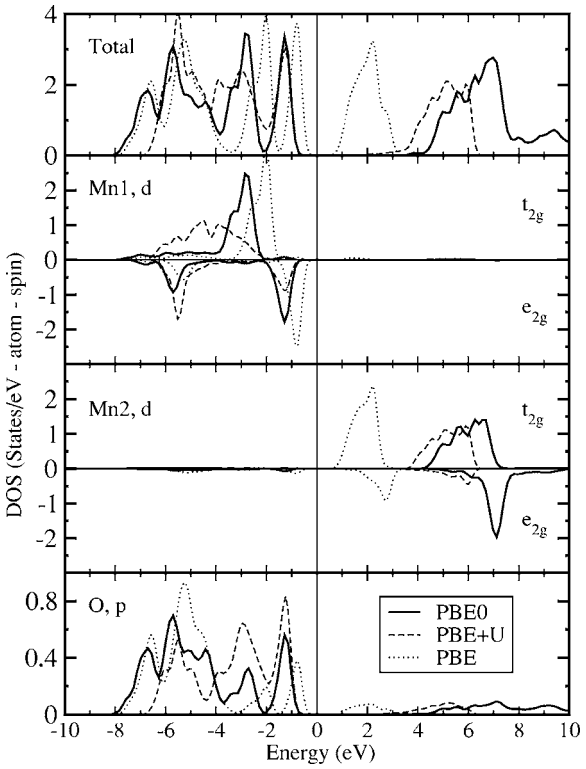

FIG. 2. DOS for MnO, calculated within three different functionals: PBE0, PBE+U, and PBE. Results for one spin component are shown.

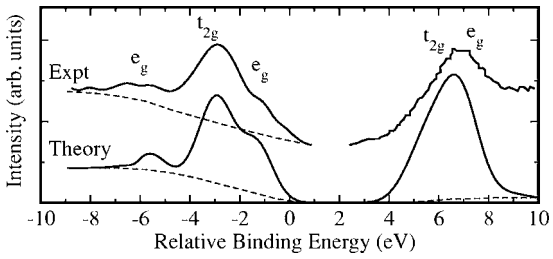

FIG. 3. Comparison between PBE0 (bottom) *d*-projected DOS of both Mn sites together with the experimental (top) inverse photoemission data (Ref. 39), and the difference between on- and off-resonance photoemission spectra (Ref. 38). Dotted lines indicate the integrated-intensity background. The levels of the experimental and calculated valence t_{2g} states have been aligned, and the calculated DOS is broadened by a convolution with a Gaussian with a width of $\sigma=0.6$ eV.

The reason for this is the intrinsic lack of the standard LSDA+U formulation which accounts only for a limited subset of electronic degrees of freedom, usually for *d* or *f* states. The Coulomb interaction for *p* is usually omitted by arguing that for fully occupied oxygen states correlation effects can be neglected. Recently, Nekrasov *et al.*[53] showed that within the LDA+U formalism a residual potential correction must be applied to the orbitals forming oxygen bands also in the fully occupied regime. Moreover, it has been shown using constrained-DFT[55] and the effective Hamiltonian method[54] that the value of the Coulomb interaction U_p for O $2p$-orbitals in strongly correlated compounds is comparable to that of the metal *d* states and plays a crucial role in understanding the bonding picture in these systems. Finally, indications exit that corrections to the Coulomb interaction on the O *p* shell arise from the self-interaction correction approach as well.[56] Therefore, we can assume that an appropriate application of LSDA+U on MnO should also take into account a shift of oxygen *p* states, on the same footing as for metal *d* states. Adding U_p to the LSDA+U treatment would shift the oxygen occupied and unoccupied *p* states apart, and by that significantly enhance the value of the gap.[53] From our PBE0 results we derive $U_p \approx 3.5$ eV, a prediction in agreement with constrained LSDA calculations, which provide $U=4.1$ eV[54] and a wide range of *U* from 3 to 8 eV.[55]

In order to stress the achievements of PBE0 in reproducing the experimentally observed properties of MnO, we show in Fig. 3 the comparison between our calculated Mn-projected DOS and photoemission and inverse photoemission data.[38,39] We stress that our results are derived within the one-particle description, where the orbital energies, with the exception of the energies of the highest occupied orbitals,[57] do not have a rigorous correspondence to excitation energies, although it has been shown that there is a surprising agreement between calculated Kohn-Sham eigenvalues and excitation energies.[58] The experimental structure at about −5.5 eV arising from bonding O $2p$–Mn e_g states as well as the shape of the t_{2g} and e_g peaks are in very good agreement with our findings and confirm the improvements of PBE0 upon conventional PBE and PBE+U.

IV. CONCLUSIONS

In summary, in this report we have shown that the admixture of 25% exact exchange with 75% of the PBE exchange functional results in a "parameter-free" hybrid functional that describes the ground state properties of MnO in excellent agreement with experiments and, when available, with the most sophisticated *ab initio* methods aiming to overcome limitations of standard local functionals. Within a PAW-DFT framework we have compared the performances of PBE0 with other PBE-based approaches (PBE, PBE+U, and HF) finding that the best description of the structural, electronic, and magnetic properties of MnO is achieved using the PBE0 method. (i) Structure: we find the most stable phase to be the rhombohedrally distorted B1 structure with a distortion angle $\alpha=0.88°$ and lattice parameter $a=4.40$ Å, (ii) magnetism: we obtain a spin magnetic moment of $m=4.52\ \mu_B$, and we derived that the structural distortion is caused by exchange striction and can be understood in terms of stronger antiparallel NN exchange interactions in comparison to parallel spin interactions, (iii) electronic structure: PBE0 reproduces well the insulating gap of 4.02 eV and the distribution of Mn $3d$ states, and places the compound MnO in the class of intermediate Mott-Hubbard/charge-transfer compounds. Although PBE0 cannot be considered strictly superior to other similar hybrid functional approaches, which have shown to describe well the nature of strongly correlated systems, its capability to reproduce many different properties with a single *a priori* fixed parameter is remarkable and holds a promise for further applications.

ACKNOWLEDGMENTS

Support from the Austrian Science Fund FWF within the Joint Research Programme S90 and the START Program is gratefully acknowledged. We thank S. Massidda and J. E. Pask for helpful and constructive discussions.

*Also at: INFM-SLACS, Sardinian Laboratory for Computational Materials Science, University of Cagliari, Italy.

[1] R. O. Jones and O. Gunnarsson, Rev. Mod. Phys. **61**, 689 (1989).
[2] L. Hedin, Phys. Rev. **139**, 796 (1965).
[3] A. Svane and O. Gunnarsson, Phys. Rev. Lett. **65**, 1148 (1990).
[4] V. I. Anisimov, J. Zaanen, and O. K. Andersen, Phys. Rev. B **44**, 943 (1991).
[5] R. L. Martin, and F. Illas, Phys. Rev. Lett. **79**, 1539 (1997).
[6] A. D. Becke, J. Chem. Phys. **98**, 1372 (1993).
[7] J. P. Perdew, M. Ernzerhof, and K. Burke, J. Chem. Phys. **105**, 9982 (1996).
[8] A. D. Becke, J. Chem. Phys. **98**, 5648 (1993).
[9] A. D. Becke, J. Chem. Phys. **104**, 1040 (1996).
[10] C. Lee, W. Yang, and R. G. Parr, Phys. Rev. B **37**, 785 (1988).

[11] I. P. R. Moreira, F. Illas, and R. L. Martin, Phys. Rev. B **65**, 155102 (2002), and references therein.
[12] X. B. Feng, Phys. Rev. B **69**, 155107 (2004).
[13] W. C. Mackrodt, D. S. Middlemiss, and T. G. Owens, Phys. Rev. B **69**, 115119 (2004).
[14] X. Feng, and N. M Harrison, Phys. Rev. B **70**, 092402 (2004).
[15] D. Munñoz, N. M Harrison, and F. Illas, Phys. Rev. B **69**, 085115 (2002).
[16] I. Ciofini, F. Illas, and. C. Adamo, J. Chem. Phys. **120**, 3811 (2004).
[17] C. Adamo and V. Barone, Chem. Phys. Lett. **274**, 242 (1997).
[18] C. Adamo and V. Barone, J. Chem. Phys. **108**, 664 (1998).
[19] M. Ernzerhof, and G. E. Scuseria, J. Chem. Phys. **110**, 5029 (1999).
[20] C. Adamo, and V. Barone, J. Chem. Phys. **110**, 6158 (1999).
[21] J. P. Perdew, K. Burke, and M. Ernzerhof, Phys. Rev. Lett. **77**, 3865 (1996).
[22] S. Chawala, G. A. Voth, J. Chem. Phys. **108**, 4697 (1998).
[23] P. E. Blöchl, Phys. Rev. B **50**, 17953 (1994).
[24] G. Kresse and D. Joubert, Phys. Rev. B **59**, 1758 (1998).
[25] G. Kresse and J. Furthmüller, Comput. Mater. Sci. **6**, 15 (1996).
[26] J. Paier, R. Hirsch, M. Marsman, and G. Kresse, J. Chem. Phys. **122**, 234102 (2005).
[27] H. Shaked, J. Faber, Jr., and R. L. Hitterman, Phys. Rev. B **38**, 11901 (1988).
[28] S. V. Faleev, M. van Schilfgaarde, and T. Kotani, Phys. Rev. Lett. **93**, 126406 (2004).
[29] S. Massidda, A. Continenza, M. Posternak, and A. Baldereschi, Phys. Rev. Lett. **74**, 2323 (1995).
[30] Z. Szotek, W. M. Temmerman, and H. Winter, Phys. Rev. B **47**, 4029 (1993).
[31] A. Filippetti and N. A. Spaldin, Phys. Rev. B **67**, 125109 (2003).
[32] M. Posternak, A. Baldereschi, S. Massidda, and N. Marzari, Phys. Rev. B **65**, 184422 (2002).
[33] S. L. Dudarev, G. A. Botton, S. Y. Savrasov, C. J. Humphreys, and A. P. Sutton, Phys. Rev. B **57**, 1505 (1998).
[34] R. N. Iskenderov, I. A. Drabkin, L. T. Emel'yanova, and Ya. M. Ksendzov, Fiz. Tverd. Tela (Leningrad) **10**, 2573 (1968) [Sov. Phys. Solid State **10**, 2031 (1969)].
[35] I. A. Drabkin *et al.*, Sov. Phys. Solid State **10**, 2428 (1969).
[36] B. E. F. Fender, A. J. Jacobson, and F. A. Wegwood, J. Chem. Phys. **48**, 990 (1968).
[37] A. K. Cheetham and D. A. O. Hope, Phys. Rev. B **27**, 6964 (1983).
[38] R. J. Lad and V. E. Henrich, Phys. Rev. B **38**, 10860 (1988).
[39] J. van Elp, R. H. Potze, H. Eskes, R. Berger, and G. A. Sawatzky, Phys. Rev. B **44**, 1530 (1991).
[40] R. W. G. Wyckoff, *Crystal Structures* (Interscience, New York, 1964).
[41] S. Massidda, M. Posternak, A. Baldereschi, and R. Resta, Phys. Rev. Lett. **82**, 430 (1999).
[42] M. D. Towler, N. L. Allan, N. M Harrison, V. R. Saunders, W. C. Mackrodt, and E. Aprá, Phys. Rev. B **50**, 5041 (1994).
[43] Z. Fang, I. V. Solovyev, H. Sawada, and K. Terakura, Phys. Rev. B **59**, 762 (1999).
[44] J. E. Pask, D. J. Singh, I. I. Mazin, C. S. Hellberg, and J. Kortus, Phys. Rev. B **64**, 024403 (2001).
[45] T. Oguchi, K. Terakura, and A. R. Williams, Phys. Rev. B **28**, 6443 (1983).
[46] T. Oguchi, K. Terakura, and A. R. Williams, J. Appl. Phys. **55**, 2318 (1984).
[47] I. V. Solovyev and K. Terakura, Phys. Rev. B **58**, 15496 (1998).
[48] M. E. Lines and E. D. Jones, Phys. Rev. **139**, A1313 (1965).
[49] M. Kohgi, Y. Ishikawa, and Y. Endoh, Solid State Commun. **11**, 391 (1972).
[50] G. Pepy, J. Phys. Chem. Solids **35**, 433 (1974).
[51] D. Hohlwein, J.-U. Hoffmann, and R. Schneider, Phys. Rev. B **68** 140408(R) (2003).
[52] B. A. Coles, J. W. Orton, and J. Owen, Phys. Rev. Lett. **4**, 116 (1960).
[53] L. A. Nekrosov, M. A. Korotin, and V. I. Anisimov, cond-mat/0009107.
[54] A. K. McMahan, R. M. Martin, and S. Satpathy, Phys. Rev. B **38**, 6650 (1988).
[55] M. S. Hybertsen, M. Schlüter, and N. E. Christensen, Phys. Rev. B **39**, 9028 (1989).
[56] M. Arai, and T. Fujiwara, Phys. Rev. B **51**, 1477 (1995).
[57] J. P. Perdew, R. G. Parr, M. Levy, and J. L. Balduz, Jr., Phys. Rev. Lett. **49**, 1691 (1982).
[58] A. Savin, C. J. Umrigar, and X. Gonze, Chem. Phys. Lett. **288**, 391 (1998).